Specific rotations of PHB in mixtures of DCA and EDC at 30 °C are plotted against the volume fraction of DCA in Figure 11. The solid curves from the present measurements show a decidedly different behavior from the dashed curve of Marchessault et al. which demonstrates an abrupt decrease in specific rotation at about 80 vol % DCA.

In Figure 12, specific rotations of PHB in a DCA–EDC mixture of 76 vol % DCA are shown as a function of temperature. The data from our measurements decrease almost linearly with the increase in temperature, whereas the dashed curve of Marchessault et al. undergoes a sharp drop at about 74 °C.

It was from the characteristic features of the dashed curves in Figures 10, 11, and 12 that these authors supposed that PHB assumes a helical conformation in such solvents as EDC, TFE, and chloroform and becomes randomly coiled in such solvents as DCA and DMF. Our polarimetric data display nothing definitive to substantiate their supposition nor give evidence that allows one to determine the actual conformation of PHB in these solvents. In such circumstances, it is reasonable to try analyzing given light-scattering and hydrodynamic data in terms of the conventional theories for nonideal solutions of random coil polymers, as has been done by a great many previous authors. In fact, we have followed this idea in the present article and have shown that, as far as light-scattering and viscosity data are concerned, the behavior of PHB in TFE is consistent with the random coil model. In the forthcoming article, we shall show that the dilute solution properties of this polymer–solvent system can be described adequately by the two-parameter theory of random coils with volume exclusion.

Acknowledgment. The authors wish to thank Professor T. Yamanaka of Osaka University and Dr. Y. Teranishi of Kyoto University for their help in the biosynthesis of PHB.

References and Notes

(1) J. M. Merrick and M. Doudoroff, *J. Bacteriol.*, **88**, 60 (1964).
(2) D. Eller, D. G. Lundgen, K. Okamura, and R. H. Marchessault, *J. Mol. Biol.*, **35**, 489 (1968).
(3) R. Alper, D. G. Lundgen, R. H. Marchessault, and W. A. Cote, *Biopolymers*, **1**, 545 (1963).
(4) K. Okamura and R. H. Marchessault, "Conformation of Biopolymers", G. N. Ramachandran, Ed., Academic Press, London, 1967, p 709.
(5) J. Cornibert and R. H. Marchessault, *J. Mol. Biol.*, **71**, 735 (1972).
(6) M. Yokouchi, Y. Chatani, H. Tadokoro, K. Teranishi, and H. Tani, *Polymer*, **14**, 267 (1973).
(7) R. H. Marchessault, K. Okamura, and C. J. Su, *Macromolecules*, **3**, 735 (1970).
(8) J. Cornibert, R. H. Marchessault, H. Benoit, and G. Weill, *Macromolecules*, **3**, 741 (1970).
(9) L. H. Stevenson and M. D. Sokolofsky, *J. Bacteriol.*, **91**, 304 (1966).
(10) H. Stockdale, D. W. Ribbons, and E. A. Dawes, *J. Bacteriol.*, **95**, 1798 (1968).
(11) R. A. Slepecky and J. H. Law, *J. Bacteriol.*, **82**, 37 (1960).
(12) D. G. Lundgen, R. Alper, C. Schnaitman, and R. H. Marchessault, *J. Bacteriol.*, **89**, 245 (1965).
(13) D. E. Agostini, J. B. Lando, and J. R. Shelton, *J. Polym. Sci., Part A-1*, **9**, 2775 (1971).
(14) L. L. Wallen and W. K. Rohwedder, *Environ. Sci. Technol.*, **8**, 576 (1974).
(15) A. H. de Mola, M. Marx-Figini, and R. V. Figini, *Makromol. Chem.*, **176**, 2655 (1975).
(16) T. Tsuji, T. Norisuye, and H. Fujita, *Polym. J.*, **7**, 558 (1975).
(17) G. C. Berry, *J. Chem. Phys.*, **44**, 4550 (1966).
(18) H. Fujita, *Polym. J.*, **1**, 537 (1970).
(19) H. Yamakawa, "Modern Theory of Polymer Solutions", Harper and Row, New York, N.Y., 1971.
(20) H. Utiyama, Y. Tsunashima, and M. Kurata, *J. Chem. Phys.*, **55**, 3133 (1971).
(21) M. Fukuda, N. Fukutomi, Y. Kato, and T. Hashimoto, *J. Polym. Sci., Polym. Phys. Ed.*, **12**, 871 (1972).
(22) J. Delsarte and G. Weill, *Macromolecules*, **7**, 450 (1974).

Compatibility in Mixtures of Poly(vinylidene fluoride) and Poly(ethyl methacrylate)

T. K. Kwei,* G. D. Patterson, and T. T. Wang

Bell Laboratories, Murray Hill, New Jersey 07974. *Received March 30, 1976*

ABSTRACT: Thermal analysis of mixtures of poly(vinylidene fluoride) and poly(ethyl methacrylate) has been carried out under a variety of controlled heating and cooling conditions. From the depression of the melting point of PVF_2 in the mixture, the binary interaction parameter is found to be −0.34, comparable to the value obtained for PVF_2–PMMA systems. Mixtures containing 80% or more PEMA are amorphous and exhibit single glass transitions. When the PEMA content is low, crystallization of PVF_2 is observed even with rapid quenching. The crystalline region coexists with two conjugate amorphous phases which contain ~100 and ~45% PVF_2, respectively. The microstructures of the blends are influenced strongly by the kinetics of phase separation and crystallization.

Mixtures of several alkyl methacrylate polymers and poly(vinylidene fluoride) have been reported to be compatible over a wide range of composition.[1-6] These compatible blends have elicited a great deal of interest from both practical and fundamental viewpoints. First, the compositions of the blends can be tailored to combine the excellent chemical resistance of polyvinylidene fluoride with the transparency of the methacrylate polymers. Second, these mixtures offer a rare opportunity for the study of the crystallization of one polymer in the presence of another.

In previous studies by several investigations, single glass transition temperatures were observed for mixtures of PVF_2 and poly(methyl methacrylate). The crystallization behavior of PVF_2 is found to be influenced significantly by the composition of the mixture as well as the rate of cooling.[3] From the melting point depression which increases with increasing PMMA content the interaction parameter between the two polymers was calculated to be −0.30 at 160 °C.[3]

An extension of the above study to mixtures of PVF_2 with poly(ethyl methacrylate) appears to be natural because it would allow us to assess the dependence of the interaction parameter on chemical structure. We also wish to reexamine the glass transition characteristics of the blends because the data of Paul and co-workers[7] indicate a single transition for each composition but the glass temperature remains nearly constant for blends containing more than 30% PVF_2. Ex-

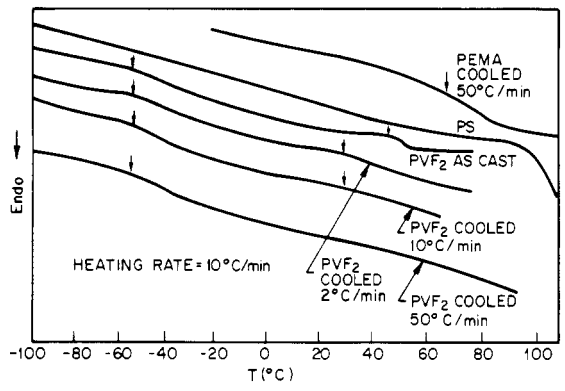

Figure 1. DSC curves of polystyrene, poly(ethyl methacrylate), and poly(vinylidene fluoride).

trapolation of their data to 100% PVF_2 yields a T_g of 33 °C which is at variance with the commonly accepted value of about −50 °C. A better understanding of the T_g behavior of these mixtures is therefore desirable.

Experimental Section

Materials. Poly(vinylidene fluoride) resin, Kynar 821, was supplied by Pennwalt Corp. in powder form. It was the same polymer as used in ref 3. The average molecular weights obtained from gel permeation chromatography are $\bar{M}_n = 2.16 \times 10^5$, $\bar{M}_w = 4.04 \times 10^5$, and $\bar{M}_z = 6.61 \times 10^5$.[8] Poly(ethyl methacrylate), prepared by suspension polymerization, was obtained from Haven Chemical Inc. The intrinsic viscosity of the PEMA in 2-butanone at 23 °C was 0.74 dl/g from which the viscosity average molecular weight was computed to be 3.91×10^5.[9] Films were cast from 3% solution in dimethylformamide using the procedure described previously.[3] For the purpose of comparison, one sample containing 80% PVF_2 was prepared by melt blending the two polymers in a Brabender Plasticorder at 180 °C for 10 min and then molding them into a sheet in a press at 150 °C. Blend compositions are reported as weight percentages throughout this paper.

Measurement of Thermal Transitions. A Du Pont Thermal analyzer, Model 990 with a DSC cell, and a Perkin-Elmer differential scanning calorimeter, Model DSC II, were used. Sample weights were 15 ± 2 mg for fusion studies. Owing to the high degree of crystallinity of PVF_2, the increase in specific heat accompanying the glass transition is small and unequivocal identification of T_g calls for more careful experimentation than is customarily necessary. To this end, the thermogram of polystyrene which was featureless from −100 to 80 °C was used for comparison. A variety of heating rates, for 5 to 50

Table I
Thermal Transitions of PVF_2–PEMA Blends Measured by Du Pont Thermal Analyzer[a]

% PVF_2	History	Heating rate, °C/min	Transition temp, °C: Below 0 °C	Transition temp, °C: Above 0 °C	T_m	ΔH Ratio
100	As cast	10	−54	48	170.6	1.0
	2 °C/min	10	−53	34 (w)	169.5	0.83
	10 °C/min	10	−53	37 (w)	165.7	0.80
	50 °C/min	10	−56		165.7	0.78
	50 °C/min	20	−55			
	Liq N_2	10	−54			
	Liq N_2	20	−53			
88.6	As cast	10	−46	38	169.5	0.80
	50 °C/min	10	−50	30	165.3	0.65
	50 °C/min	20	−54	27		0.65
	Liq N_2	10	−50	15* cryst 28	165.0	
	Liq N_2	20	−54	18* cryst 24		
80	As cast	10	−45	24	168.1	0.71
	50 °C/min	10	−51	25	165.3	0.58
	50 °C/min	20	−54	26		
	Liq N_2	10	−48, −19 (vw)	17* cryst 30	162.8	
80	Milled	10	−40	30	166.1	
	50 °C/min	10	−50	28	165.6	
77.2	As cast	10			167.5	0.65
	50 °C/min	10			163.3	0.53
70	As cast	10	−46	38	165.5	0.63
	50 °C/min	10	−50	30	162.5	0.50
	50 °C/min	20	−54	28		
	Liq N_2	10	−52, −10	Cryst 0	162.0	
	Liq N_2	20	−52, −19	5* cryst 27		
60	As cast	10	−42	42	162.2	0.51
	50 °C/min	10	−52	10, cryst 40	161.0	
	50 °C/min	20	−50	14, cryst 40		
	Liq N_2	10	−50	10, cryst 40	160.7	
58.7	As cast	10			161.9	0.47
48	As cast	10	−42	22	158.5	0.42
	50 °C/min	10		25	157.5	0.025
	50 °C/min	20		26		
	Liq N_2	20		30		
40	As cast	10	−42	42	155.8	
	2 °C/min	10		35	NC	
	50 °C/min	10		32	NC	
	50 °C/min	20		32	NC	
20	As cast	10		50	NC	
	As cast	20		50	NC	
0	As cast	10		62		
	As cast	20		65		
	50 °C/min	10		64		
	50 °C/min	20		67		

[a] NC = noncrystalline; w = weak; vw = very weak.

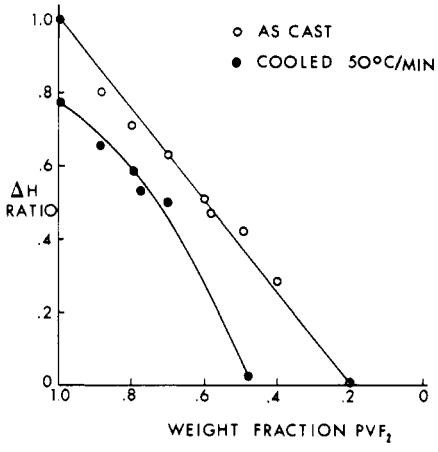

Figure 2. ΔH ratios of PVF_2–PEMA mixtures.

°C/min, were employed although a majority of experiments were conducted at heating rates of 10 and 20 °C/min, respectively. Different sample sizes were tried and a weight of 20 to 25 mg was found to be suitable for our purpose. The uncertainty in T_g measurement is ±2 °C unless otherwise stated. Typical thermograms are shown in Figure 1.

The thermal histories of the films were varied by maintaining the samples in the DSC cell at 180 °C for 10 min followed by cooling at a constant rate. In several experiments, a melted film in a sample pan was removed from the DSC cell and immersed directly in liquid nitrogen. A stream of nitrogen gas was used to dry the sample pan which was then placed immediately back in a DSC cell precooled to −120 °C.

Results

Fusion. The melting endotherms of blends of PVF_2 with PEMA are similar to those reported previously for PVF_2–PMMA and therefore are not shown here. The melting temperatures, T_m, are generally reproducible to ±0.5 °C and are in good agreement with the results of Paul.[7] The small differences, less than 1 °C, between the two sets of data can be attributed to the different methods of sample preparation. As-cast film containing 40% or more PVF_2 is crystalline but the 20% PVF_2 film is not. Although the melting temperature identified by a DSC experiment is not an equilibrium value, the magnitude of melting point depression which is our primary concern is generally believed to be reasonably accurate. The melting point data are recorded in Table I, in which the last column gives the ratio of the endothermic area per gram of film to that of the as-cast PVF_2. The ΔH ratios decrease linearly with decreasing PVF_2 concentration in the as-cast films (Figure 2).

Glass Temperatures. The T_g of PEMA is between 62 and 67 °C and can be detected without difficulty (Figure 1). The glass transition of PVF_2 occurs at about −54 °C, in accordance with literature values. The change in specific heat is small and the transition is broad. In addition to the glass transition, the thermogram of the as-cast PVF_2 film exhibits a baseline shift (endothermic) at 48 °C (Figure 1). This endothermic response was designated as an "upper glass transition", T_g(U), by Paul but we wish to reserve judgment on their interpretation. The presence of this endothermic event, however, interferes with the identification of the T_g of blends which also show endothermic responses in the same temperature range. One cannot be certain that any transition occurring near 40 °C in the blends is originated from lowering of the T_g of PEMA as a result of mixing with PVF_2, rather than from PVF_2 itself. Therefore we attempted to vary the thermal history of PVF_2 in the hope of altering its response in this temperature range. Films cooled at 2 and 10 °C/min from the melt showed endothermic responses at 32 °C which were eliminated when the cooling rate was increased to 50 °C/min or higher. These curves are also shown in Figure 1. Consequently, we believed

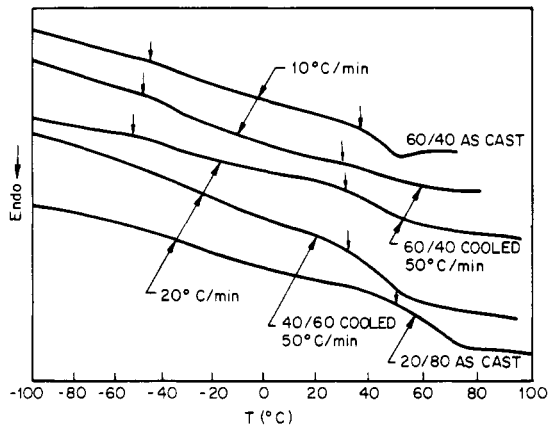

Figure 3. DSC curves of PVF_2–PEMA mixtures. Compositions are expressed as the weight ratio of PVF_2 to PEMA. Heating rates are indicated for each scan.

Table II
Low-Temperature Transitions of PVF_2–PEMA Blends Determined by Perkin-Elmer DSC II

% PVF_2	Cooling rate, °C/min	Heating rate, °C/min	T_g, °C
100	320	40	−60 ± 5
88.6	320	40	−60 ± 5
80	320	40	−70 ± 5
70	320	40	−60, −20
60	320	40	−60, 10
48	320	40	30
0	320	40	69

that it was advantageous to compare the thermograms of quenched films.

Quenched films containing 60% or more PVF_2 exhibited more than one glass transition. Common to these films was the transition near −50 °C which could always be detected at a variety of cooling and heating rates. The location of the second or third transition depended strongly on the thermal history of the sample. In several cases, the onset of crystallization near room temperature overlaps the transitions in the same region. These overlapped transitions which cannot be identified with confidence are denoted by asterisks in Table I. Two glass transitions were also detected, at −40 and 30 °C, respectively, for the melt-blended sample containing 80% PVF_2, in general agreement with the results found for the solvent cast film of the same composition.

The best resolution of the many thermal transitions was achieved, with the Du Pont instrument, at a cooling rate of 50 °C/min and a heating rate of 20 °C/min. Representative thermograms are shown in Figure 3. Quenching in liquid nitrogen did not result in a single transition for these compositions; instead, the thermograms became more complex.

When the weight percent of PVF_2 was less than 48% in the mixture, only one transition was observed for the quenched material (Figure 3). The as-cast film containing 20% PVF_2 was not crystalline and exhibited a single T_g. The T_g data are recorded in Table I.

Since it was crucial to establish beyond doubt the existence of the low-temperature transition near −50 °C a second instrument, a Perkin-Elmer DSC II, was used to confirm the results obtained with the Du Pont thermal analyzer. A quenching rate of 320 °C/min and a heating rate of 40 °C/min were employed. The low-temperature transition characteristic of PVF_2 was always prominent for mixtures containing 60% or more PVF_2 (Table II). The data for 60 and 70% PVF_2 films were in excellent agreement with the results obtained with the

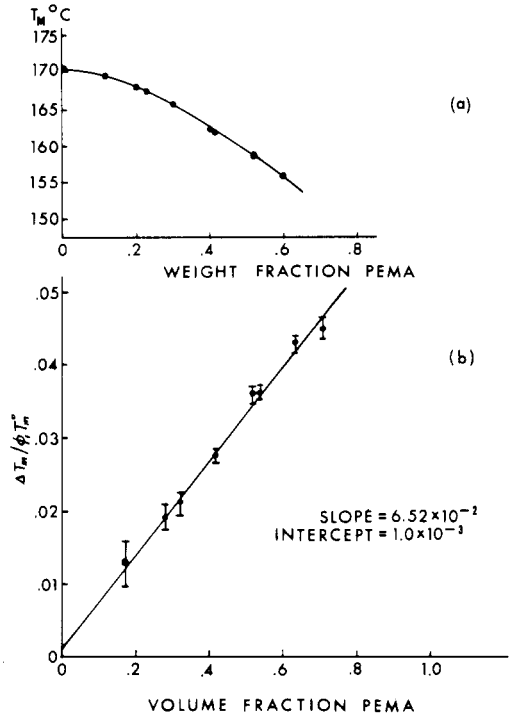

Figure 4. Melting point depression of PVF_2.

Du Pont instruments for the same films quenched in liquid nitrogen. The presence of the transition near −55 to −60 °C in PVF_2-rich films was therefore firmly established.

Discussion

(1) Melting Temperature. In the study of Nishi and Wang, the melting temperature of a crystalline polymer (component 2) in the presence of a polymeric diluent (component 1) was analyzed using Scott's expression[10] for chemical potentials in a binary polymer mixture. The resulting equation for melting temperature depression is,[3]

$$\frac{\Delta T_m}{T_m^0} = -\frac{\bar{V}_{2u} B_{12}}{\Delta H_{2u}} \phi_1^2 \qquad (1)$$

where T_m^0 is the melting temperature of the undiluted crystalline polymer, ΔT_m is the lowering of melting point, ϕ is the volume fraction of the polymeric diluent, $\bar{V}_{2u}$ and ΔH_{2u} are the molar volume and heat of fusion per segment, and B_{12} is related to the binary interaction parameter by the equation,[11]

$$\chi'_{12} = \chi_{12}/x_1 = B_{12}\bar{V}_{1u}/RT \qquad (2)$$

Here χ_{12} is the Flory interaction parameter, x is the number of segments, and $\bar{V}_{1u}$ is the molar volume per unit of component 1. (We prefer to use χ'_{12} to avoid future confusion; χ_{12} in ref 3 is identical with χ'_{12} in this paper.)

A convenient graphical representation of melting point data makes use of the plot of $\Delta T_m/\phi_1 T_m^0$ vs. ϕ_1. This is shown in Figure 4. The experimental results are represented by a straight line which intersects the ordinate axis near zero, as predicted by eq 1. From the slope of the straight line, we obtain ($\bar{V}_{2u}$ = 36.4 cm³/mol, ΔH_{2u} = 1.6 kcal/mol, $\bar{V}_{1u}$ = 101.9 cm³/mol),

$$B_{12} = -2.86 \text{ cal/cm}^3 \text{ of PEMA}$$

$$\chi'_{12} = -0.34 \text{ at } 160\ ^\circ\text{C}$$

The negative sign of B_{12} indicates that the polymer pair can form thermodynamically stable single-phase mixtures at temperatures near the melting point of PVF_2. The magnitude of B_{12} agrees rather well with the result of Paul[7] and is nearly identical with the value of −2.98 obtained for PVF_2–PMMA.[3] The addition of a methylene group to the side chain of the methyl methacrylate polymer does not seem to have a significant influence on its compatibility with PVF_2 at elevated temperatures.

The possibility exists that the depression in melting point may also arise from morphological changes such as imperfections in the crystals and reduction in lamellar thickness. However, some clues can be found in the study by Nishi and Wang[3] who conducted extensive investigation of the crystallization and fusion characteristics of PVF_2–PMMA mixtures. In their study of isothermally crystallized samples, a linear relationship was observed between T_m and T_c, the crystallization temperature. The stability parameter ϕ, which was in fact a morphological parameter, was independent of composition. This would not be the case if the melting point depression was mainly a result of morphological changes. This conclusion is probably applicable to the present system although we have not performed similar experiments.

(2) Glass Transitions. An obvious conclusion to be drawn from the observation of the melting endotherm described in the preceding section is the presence of crystalline regions in many mixtures. In this section we direct our discussion to the amorphous phases. Although PVF_2 and PEMA are compatible at elevated temperatures, as indicated by a negative value of the interaction parameter, compatibility should not be taken for granted at lower temperature for all compositions because an upper critical solution temperature may exist for the mixtures. The data in Table I indicate single glass transitions only for PEMA-rich mixtures. Blends containing 60% or more PVF_2 exhibit more than one transition even in the quenched state. For the moment, we shall focus our attention on the T_g data for these films ($PVF_2 \geq 60\%$) cooled from the molten state at 50 °C/min to −120 °C and heated at 20 °C/min (Figure 3). The low-temperature transition which occurs near −50 °C in each mixture suggests the presence of an amorphous phase comprised of nearly pure PVF_2. Correspondingly, the higher temperature transitions must arise from segmental motions of phases relatively rich in PEMA. Therefore, the microstructure of these films can be depicted as a composite of crystalline regions coexistent with two amorphous phases.

From the above discussion, it is expected that the compositions of the two amorphous phases remain the same, at equilibrium, regardless of the initial composition of the film. We have already indicated that one of the phases always consists of nearly 100% PVF_2. The composition of the second phase can be estimated from the locations of the upper T_g's, namely, 27, 26, 28, and 14 °C for the 88.6, 80, 70, and 60% PVF_2 films, respectively. Except for the 60% film which shows recrystallization near 40 °C and will be discussed further in a later section, the variation in T_g is within experimental error. Therefore we conclude, as a first approximation, that the second amorphous phase in these films indeed has a constant composition, in accordance with the requirement of conjugate phases.

If the T_g of the second amorphous phase is taken as ~27 °C, then the phase composition is estimated to be about 45% PVF_2, from Figure 5. (Only about 5% of the PVF_2 in the 48% PVF_2 film crystallized while the 40% PVF_2 film is noncrystalline.) The probable shape of the phase diagram is given in Figure 6. The phase diagram predicts stable, signle-phase structure at room temperature when the PEMA content in the quenched film is in excess of 55%. The single-phase character is expected to be retained even at temperatures below the phase boundary because the rate of phase separation becomes negligible below T_g. Thus, the major features of the T_g behavior of the blends are embodied in Figure 6.

In comparing our data with those by Paul and co-workers,

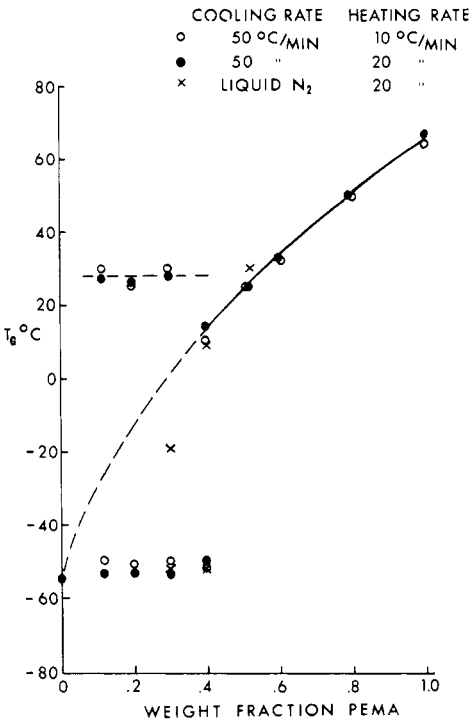

Figure 5. Glass transition temperature of PVF_2–PEMA mixtures.

the similarity of their results with the high-temperature portion of Figure 5 is evident. It is difficult to ascertain the reason for the divergence of low-temperature observations but we recognize the differences in the molecular weights of the polymers and in the thermal histories of the samples used in the two studies. The two transitions detected in our as-cast films may also be real although the arguments used for the phase relationship in a binary system cannot be transferred directly to precipitation in a ternary mixture containing a solvent. It may be mentioned in passing that the T_g data of the as-cast PVF_2–PMMA films[3] can perhaps be rationalized in a similar manner.

Aside from the various approximations used to arrive at Figure 6, the proposed diagram is useful only for the prediction of phase composition at equilibrium. At very high quenching rates, for example, immersion in liquid nitrogen, the kinetics of phase separation may dominate. Incomplete phase separation manifests itself in more than two glass transitions in several cases. Furthermore, the rates of phase separation and crystallization are also dependent on composition. The observation that the high-temperature transition for the 60% PVF_2 film cooled at 50 °C/min appears to correspond to phase composition somewhat inside the phase boundary of Figure 6 reflects incomplete phase separation and crystallization under the experimental conditions. This is confirmed by the crystallization phenomenon at 40 °C upon heating. The uncrystallized PVF_2 trapped with PEMA lowers the T_g of the second amorphous phase to 14 °C, instead of the predicted value of 27 °C.

Finally, we address briefly the different behaviors of PMMA and PEMA blends with PVF_2. The former can be quenched more readily to a single phase, noncrystalline structure. The difference in crystallization rate may be ascribed in part to the large difference in the viscosities of the

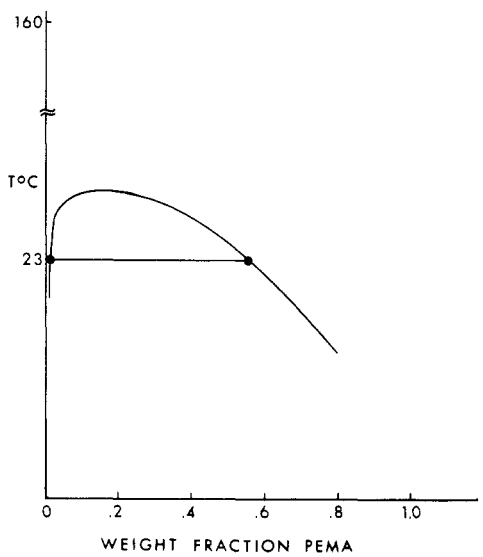

Figure 6. Proposed phase diagram.

two methacrylate polymers at the crystallization temperature. Although PEMA has a higher molecular weight it has a lower melt viscosity at 170 °C, 1×10^5 vs. 3.4×10^5 P at a shear rate of 10 s^{-1}, because its T_g is lower. At a crystallization temperature of about 130 °C, the viscosity of PMMA is too high to be measured by capillary rheometer.

Conclusion

PVF_2 and PEMA form stable single-phase mixtures in the melt. The binary interaction parameter is −0.34 at 160 °C, comparable to the value for PVF_2–PMMA blends. Mixtures containing 80% or more PEMA are amorphous and exhibit single glass transitions. When the PEMA content is below 40%, crystallization of PVF_2 prevails even at high cooling rates. In addition, two conjugate amorphous phases, one consisting of nearly 100% PVF_2 and the other about 45%, are present. The microstructures of these mixtures are influenced strongly by the kinetics of phase separation and crystallization.

Acknowledgment. We are grateful to Mrs. M. Y. Hellman and Mr. C. Gieniewski for their contributions in molecular weight and melt viscosity determinations. We also wish to acknowledge many valuable and stimulating discussions with Drs. E. Helfand, D. C. Douglass, V. J. McBrierty, and H. L. Frisch. Thanks are also due to Professor D. R. Paul for sending us his manuscript before publication.

References and Notes

(1) J. S. Noland, N. N. C. Hsu, R. Saxon, and J. M. Schmitt, *Adv. Chem. Ser.*, **No. 99**, 15 (1971).
(2) D. R. Paul and J. O. Altamirano, *Polym. Prepr., Am. Chem. Soc., Div. Polym. Chem.*, **15**, 409 (1974).
(3) T. Nishi and T. T. Wang, *Macromolecules*, **8**, 909 (1975).
(4) F. F. Koblitz, R. G. Petrella, A. A. DuKert, and A. Christofas, U.S. Patent 3 253 060 (1966).
(5) C. H. Miller, Jr., U.S. Patent 3 458 391 (1969).
(6) J. M. Schmitt, U.S. Patent 3 459 834 (1969).
(7) R. L. Imken, D. R. Paul, and J. W. Barlow, in press.
(8) M. Y. Hellman, private communication.
(9) S. N. Chinai and R. J. Samuels, *J. Polym. Sci.*, **19**, 463 (1956).
(10) R. L. Scott, *J. Chem. Phys.*, **17**, 279 (1949).
(11) P. J. Flory, "Principles of Polymer Chemistry", Cornell University Press, Ithaca, N.Y., 1953.